

THE CONDITION OF STRESS AND STRAIN OF HIGH AND MEDIUM STRENGTH METAL SHEET AT CRACK INITIATION

CHINMAYA BISWAL
MECHANICAL DEPARTMENT, CUTTACK

Abstract

Strain and stress conditions in sheet metal shearing are of enthusiasm for adjustment of different crack criteria. Most break criteria are administered by successful strain and stress triaxiality. This work is an endeavor to expand past estimations of strain fields in shearing of steel sheets with the pressure state determined from the deliberate removal fields. Results are introduced as far as von Mises pressure and stress triaxiality fields, and an examination was made with limited component reenactments. Additionally, an assessment of the similitudes of the pressure conditions on the sheet surface and inside the mass material was presented. Strains and von Mises stresses were like the surface and the mass material, yet the pressure triaxiality was not practically identical. There were huge inclinations in strain and worry around the bended instrument profiles that made the outcome goals ward and examinations of greatest strain and stress esteems difficult. The push state on the sheet surface determined from relocation field estimations is valuable for approval of a three-dimensional limited component display.

Catchphrases: Sheet metal, Experiment, Shearing, Strain, Stress, Crack commencement

Introduction

Shearing is a typical procedure in the sheet metal Indus attempt. The consistent improvement of new sheet materials with different shearing properties makes it alluring to have a model of the shearing procedure that can anticipate the appropriate shearing parameters. That show must think about the break notwithstanding the huge plastic miss hapenings. Various crack criteria, in light of strain and stress conditions, exist which can be utilized in limited component (FE) models of the shearing, for instance, most extreme compelling strain, greatest shear pressure, or joined anxiety criteria (Cockcroft and Latham 1968; Johnson and Cook 1985). Such criteria should be aligned against tentatively estimated strain and stress conditions. The malleable crack is all in all administered by powerful strain and stress triaxiality as seen by McClintock (1968). Low triaxiality results in shear dimple crack while high triaxiality results in void mixture as demonstrated by Rice and Tracey (1969).

Strain and stress conditions can be determined from full-field estimations of dislodging as appeared by Marth et al. (2016). In that work, gradual uprooting fields were acquired from caught pictures amid the experi-ments by the computerized picture connection (DIC) method, intensive looked into by Hild and Roux (2006). With DIC, the relocations are estimated on sub-pixel level, see for instance Sjö Dahl (1994). Precision in DIC estimations are canvassed in detail by Sjö Dahl (1997).

Strains were estimated amid planar blanking by Stegeman et al. (1999) and in trials with a sym-metric shearing set-up by Gustafsson et al. (2016b). The reason for the present work was to expand these analyses with pressure computations utilizing the technique portrayed by Marth et al. (2016), to decide the strain and stress conditions at break commencement.

Shearing test

The shearing tests were performed with the technique and set-up created by Gustafsson et al. (2014). This set-up utilizations symmetry to adjust the power characterized as F_x in Fig. 1. In this manner, no aides with erosion misfortunes are required, and the powers, F_x and F_y , which are estimated in the set-up, are precise. The structure likewise includes extensive solidness in the x-bearing and therefore a steady device clear-ance c. Apparatus removals, U_x and U_y , were estimated with straight transducers as depicted by Gustafsson et al. (2016a). Device freedom and cinching of the sheet tests were differed in the analyses: clearances 0.05h, 0.15h and 0.25h, where h is the sheet thickness utilized and the sheet was braced on one or the two sides as appeared in Fig. 1. Pictures of the around amplified region appeared in Fig. 1 were caught amid the shearing to enlist the in-plane misshapening of the sheet. For this reason, the xy-surface of the sheet tests was set up with a ran-dom spot design for consequent advanced picture correla-tion. Further subtleties on the examinations are portrayed by

Gustafsson et al. (2016b).

Picture investigation and strain assessment

The computerized picture connection (DIC) system, imple-mented with the business programming ARAMIS, was utilized to

figure the disfigurement angles at first glance. The assessed region was divided into sub-regions, called aspects, and afterward, these features were followed through cross-connection of the pictures caught amid the shearing. The feature estimate was 64×64 pixels, and the aspect step measure was 8 pixels toward every path. The in-plane strain field (x-and y-parts) was determined from the deliberate disfigurements, and under suspicion of plastic incompressibility, the missing strain segment (z-bearing) was determined, as appeared by Kajberg and Lindkvist (2004).

Table 1 Mechanical properties in terms of yield strength Rp02, tensile strength Rm and elongation A80, evaluated from uniaxial tensile tests of sheet metal grades used in the study

Material	Rp02	Rm	A80	<i>h</i>	<i>K</i> [MPa]	<i>n</i>
strengt <i>h</i>	[MPa]	[MPa]	[%]	[mm]		[—]
Mediu m	450	520	25	5.97– 6.03	880	0.12 7
High	1080	1260	7	6.11– 6.15	155 0	0.03 45

The range of sheet thickness *h* for the sheared samples is also shown.

Evaluation of stress from measured strain

The strain tensor, obtained as described in previous sub-section, was used to calculate the stress tensor by a radial return algorithm based on isotropic von Mises plasticity, as described by Marth et al. (2016), but without using a stepwise modelling of the hardening relation. Instead of this stepwise modelling, the plastic work hardening of the materials was modelled with the Hollomon hardening law using the material parameter presented in Table 1. From the stress tensor, the effective von Mises stress was calculated as

$$\bar{\sigma} = \frac{\sqrt{3}}{2} s_{ij}s_{ij},$$

where $s_{ij} = \sigma_{ij} - \sigma_{kk}\delta_{ij}/3$ is the deviatoric stress tensor. Taking the mean stress, $\sigma_m = \sigma_{kk}/3$

Since the strain values used in this method were obtained on the material surface, a plane stress approach was used to evaluate the surface stress conditions. A

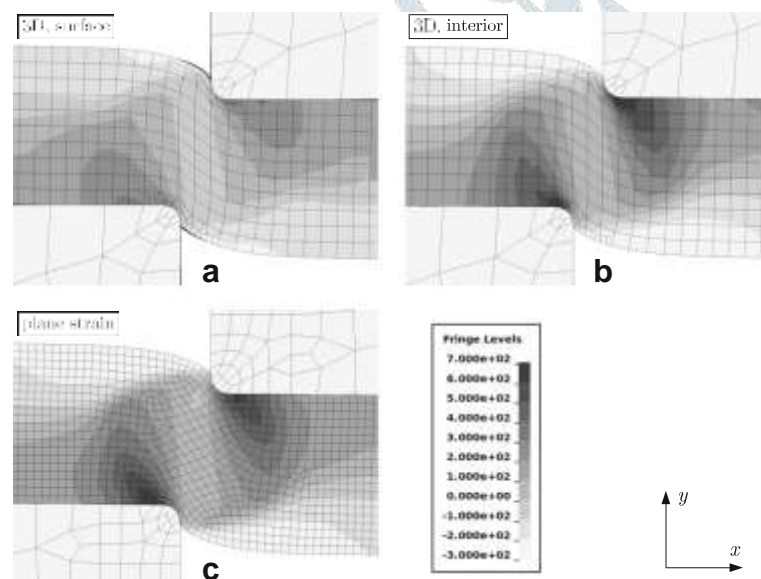


Fig. 2 Pressure, $-\sigma_{kk}/3$, fields from generic 3D and plane strain simulations. Fringe levels are in megapascal. **a** 3D, surface. **b** 3D, interior. **c** plain strain

Finite element simulations

Plane strain FE analyses of the shearing were performed with a commercial general-purpose finite element software. Geometry and boundary conditions for the model

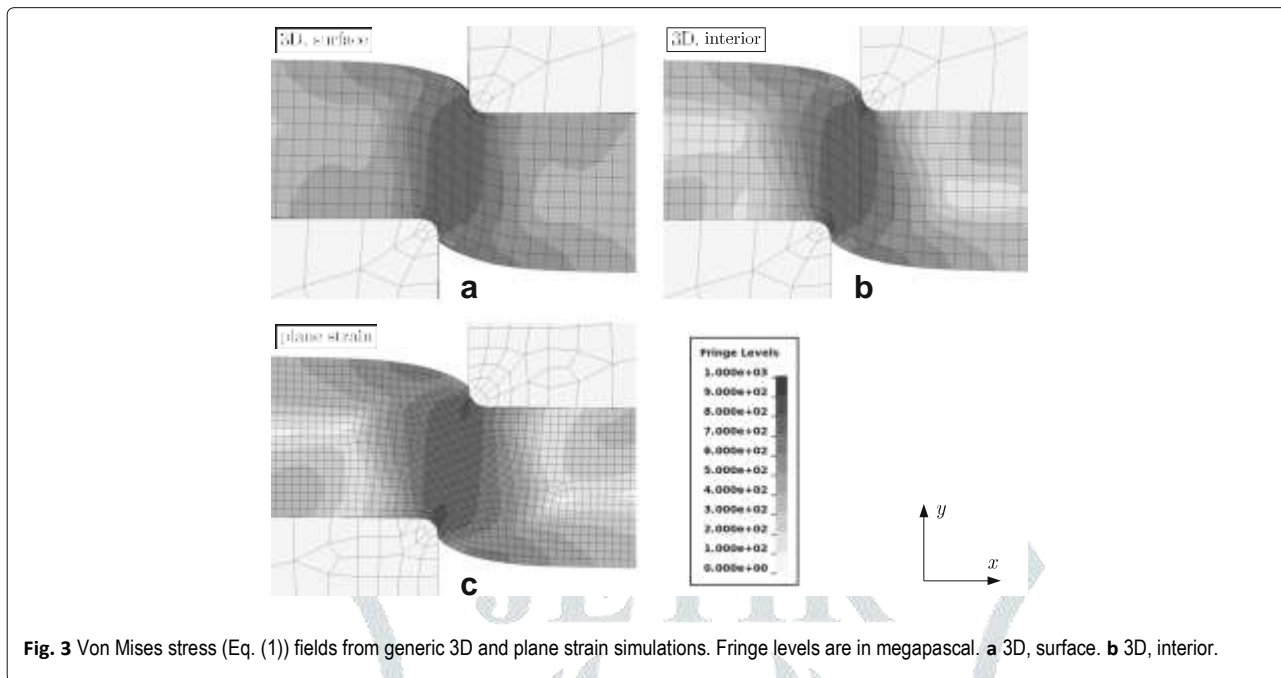


Fig. 3 Von Mises stress (Eq. (1)) fields from generic 3D and plane strain simulations. Fringe levels are in megapascal. a 3D, surface. b 3D, interior.

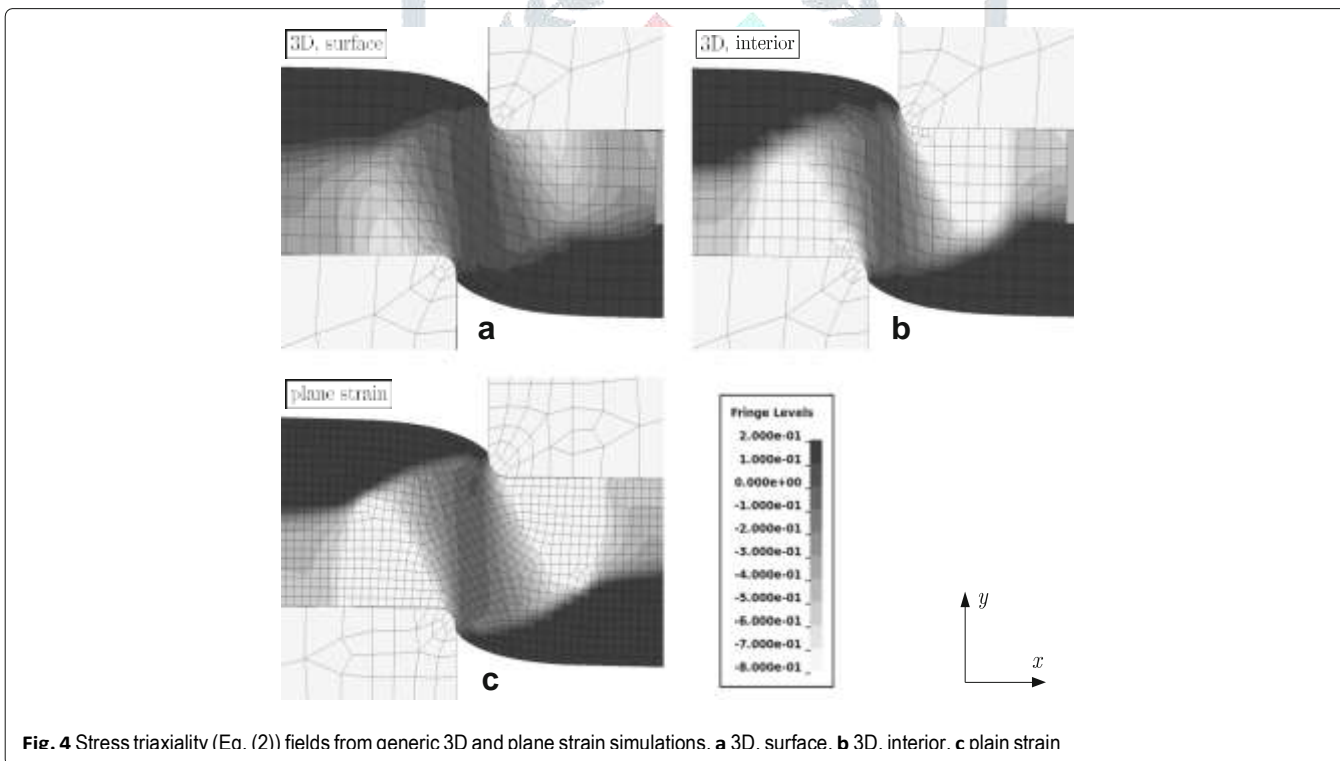


Fig. 4 Stress triaxiality (Eq. (2)) fields from generic 3D and plane strain simulations. a 3D, surface. b 3D, interior. c plain strain

Comparison between experiments and simulations

Comparisons were made between results from FE simulations and results based on measurements, in terms of effective von Mises stress (Eq. (1)) and stress triaxiality (Eq. (2)). Furthermore, effective strain and tool forces versus tool displacement were presented for comparison with corresponding experimental data presented by Gustafsson et al. (2016b). An agreement between these simulations and experiments (effective strain and force vs. displacement) should be seen as a validation of the FE model. The effective plastic strain fields from the FE simulations

$$\bar{\epsilon}_p = \int \sqrt{\frac{2}{3} D_{ij}^p D_{ij}^p} dt, \tag{3}$$

where D_p

ij is the plastic component of the rate of deformation tensor, which can be compared with the effective strains measured by Gustafsson et al. (2016b), since the elastic part of the latter is negligible.

All presented strains and stresses are from the stage of crack initiation. The fracture was not modelled in the FE simulations, and a comparison with experiments is therefore irrelevant after crack initiation.

Results

To begin with, results from conventional FE recreations are exhibited to indicate how the pressure state fluctuates between the surface and the mass material, and that plane strain is a tasteful guess of the conditions in the mass material ("Generic FE reproductions of the pressure state" area). Second, the FE model of the test shearing conditions is approved against recently distributed device powers and strain fields ("Validation of the FE demonstrate at experimen-tal conditions" area). Third, a correlation between the pressure state from FE recreations and from figurings dependent on the deliberate dislodging fields is exhibited, as far as compelling von Mises pressure ("Comparison of von Mises pressure" area) and stress

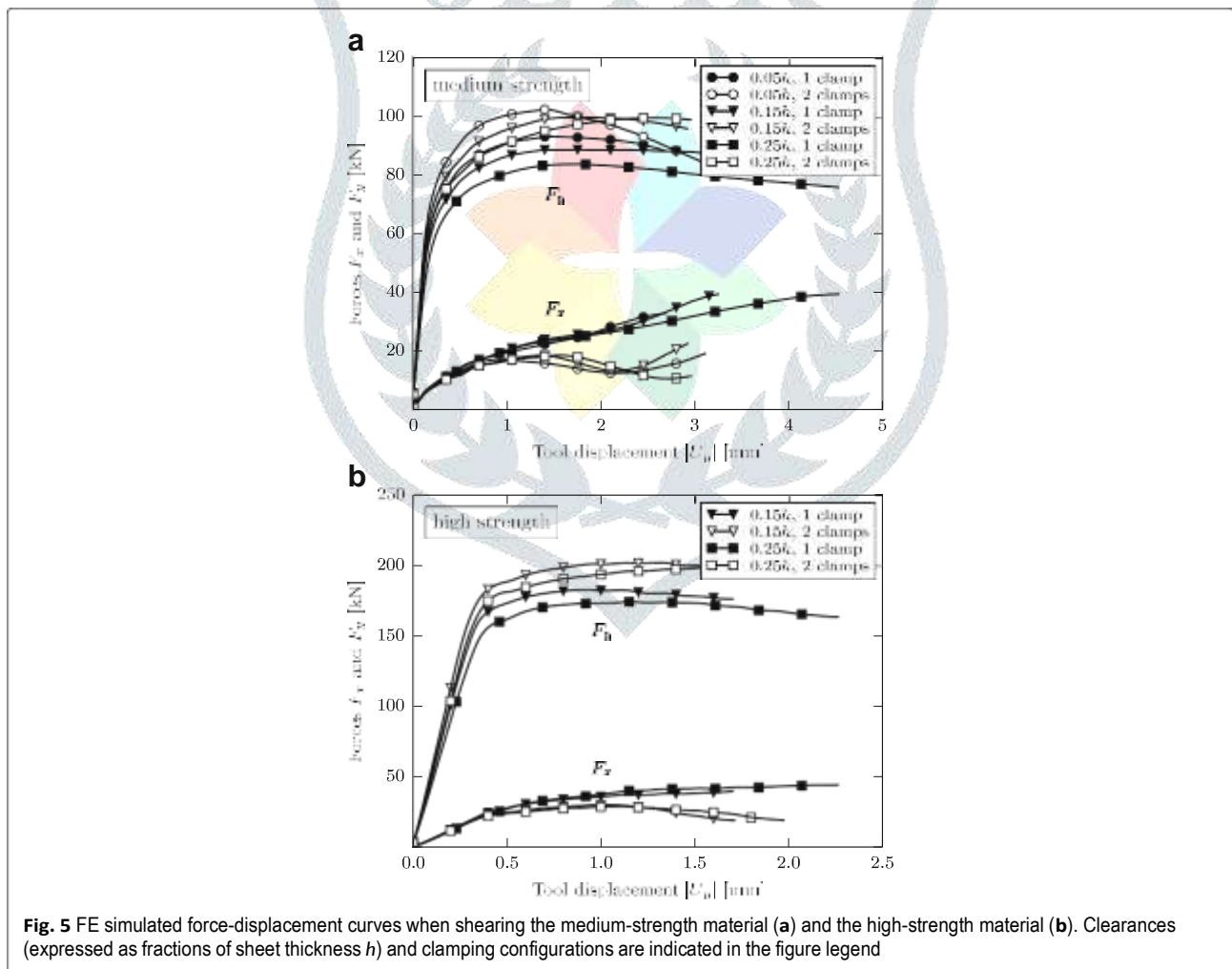


Fig. 5 FE simulated force-displacement curves when shearing the medium-strength material (a) and the high-strength material (b). Clearances (expressed as fractions of sheet thickness h) and clamping configurations are indicated in the figure legend

triaxiality ("Comparison of stress triaxiality" area). The pressure determined from estimated relocation fields will in the future be alluded to as exploratory pressure. At long last, a synopsis of the examination among reproduced and tentatively based anxiety conditions shuts this segment ("Summary of estimated and recreated results" segment).

Validation of the FE model at experimental conditions Tool forces from the FE simulations, up to the tool displacement $|U_y|$ where final fracture occurred in the experiments, are presented in Fig. 5.

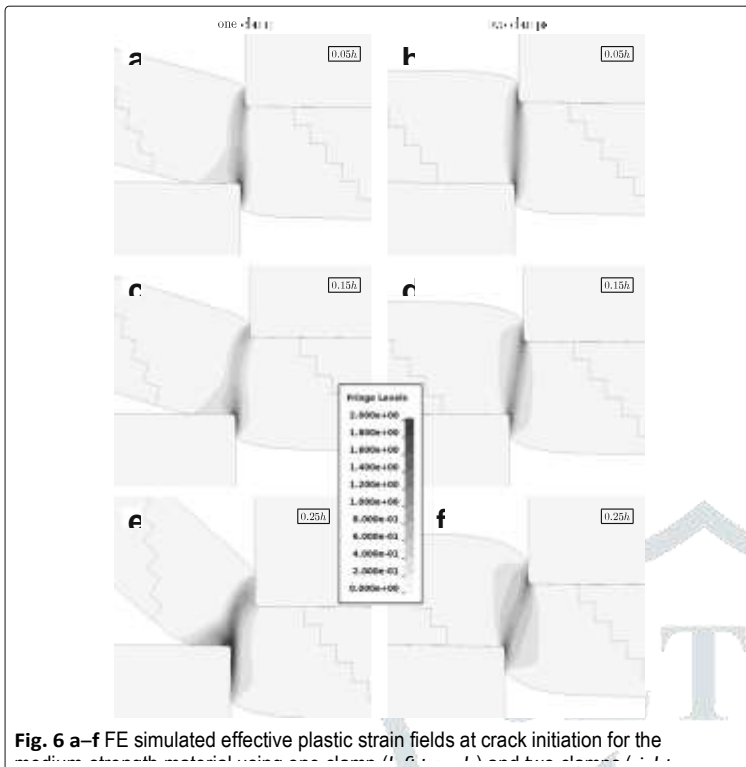


Fig. 6 a-f FE simulated effective plastic strain fields at crack initiation for the two different strength material grades with one clasp (600 MPa) and two clips (700 MPa).

Conclusions

The anxiety conditions at split inception in shearing of two steel sheet grades with different freedom and clamping were examined by estimations dependent on measured removal fields and by limited component simulations. The limited component show was first approved against tentatively estimated instrument powers and strain fields on the sheet surface. Ends from the investigation were as per the following:

- Effective strains and vonmises stresses were like the sheet surface and inside the mass material. Mean pressure, and thusly likewise triaxiality, was anyway not tantamount at first glance and inside the material.

There were vast slopes in strain and worry around the bended instrument profiles that were not caught by the exploratory strategy. The outcomes are as yet helpful in blend with limited component reproductions that are first approved with the exploratory information and later used to give missing information of anxiety at the sheet edges.

- Slightly bigger viable strains and von Mises stresses were by and large observed when shearing with one clasp contrasted and two clips, however no reasonable pattern was seen for the pressure triaxialities

References

- Cockcroft, MG, & Latham, DJ (1968). Ductility and the workability of metals. *Journal of the Institute of metals*, 96(1), 33–39.
- Gustafsson, E, Oldenburg, M, Jansson, A (2014). Design and validation of a sheet metal shearing experimental procedure. *Journal of Materials Processing Technology*, 214(11), 2468–2477.
- Gustafsson, E, Karlsson, L, Oldenburg, M (2016a). Experimental study of forces and energies during shearing of steel sheet with angled tools. *International Journal of Mechanical and Materials Engineering*, 11(1), 10.
- Gustafsson, E, Karlsson, L, Oldenburg, M (2016b). Experimental study of strain fields during shearing of medium- and high-strength steel sheet. *International Journal of Mechanical and Materials Engineering*, 11(1), 14.